ELSEVIER

Materials Science and Engineering A 459 (2007) 151–155

MATERIALS SCIENCE & ENGINEERING A

www.elsevier.com/locate/msea

In situ observations of sigma phase dissolution in 2205 duplex stainless steel using synchrotron X-ray diffraction

J.W. Elmer [a,*], T.A. Palmer [a], E.D. Specht [b]

[a] *Lawrence Livermore National Laboratory, Livermore, CA, United States*
[b] *Oak Ridge National Laboratory, Oak Ridge, TN, United States*

Received 10 August 2006; received in revised form 19 December 2006; accepted 11 January 2007

Abstract

Synchrotron radiation was used to directly observe the transformation of ferrite, austenite and sigma phases during heating and cooling of 2205 duplex stainless steel. Sigma formed during the initial stages of heating, dissolved as the temperature was increased, and reformed on cooling. The dissolution temperature of sigma was measured to be 985 ± 2.8 °C at a heating rate of 0.25 °C/s, and the kinetics of sigma formation at 850 °C was determined to be slower after dissolving at 1000 °C than before.
© 2007 Elsevier B.V. All rights reserved.

Keywords: Synchrotron; *In situ* diffraction; Duplex stainless steel; Sigma phase; Ferrite; Austenite; Transformation kinetics; Thermodynamic calculations; Dissolution temperature

1. Introduction

Undesirable phases are known to form in duplex stainless steel (DSS) alloys when they are exposed to temperatures between approximately 600 and 1000 °C for sustained periods of time [1]. These phases include σ, χ, and π, with σ phase being the most prominent [2,3]. Sigma phase has a complex tetragonal crystal structure with a large unit cell and is enriched in Cr and Mo relative to the nominal composition of the alloy [4]. Sigma is known to adversely affect the mechanical properties [4,5] and corrosion resistance [6,7] of DSS alloys.

Prior investigations have shown that sigma nucleates preferentially at austenite/ferrite boundaries or at ferrite/ferrite grain boundaries, and grows into the ferrite which is enriched in the sigma forming elements [1–4]. Sigma has been observed in both wrought [1–4] and cast alloys [8,9], in weld metal fusion and heat affected zones [10,11], and in continuously cooled DSS alloys [12], indicating its propensity to form under numerous materials processing conditions.

In this investigation, *in situ* X-ray diffraction is used to observe the formation, growth and dissolution of σ phase during a controlled heating cycle that peaks at 1000 °C. These types of synchrotron studies have a number of inherent advantages over more conventional optical metallographic techniques since microstructural changes can be monitored in real time to provide a continuous measurement of the transformations as they occur. Along with the formation and growth of the σ phase, the formation and growth of secondary austenite and the transformation of ferrite were observed and measured in real time. Results from this work provide a basis for more in-depth investigations of the transformation kinetics involved with σ phase formation and dissolution in DSS alloys.

2. Experimental procedures

2.1. Material properties

Chemical analysis performed on the 2205 DSS used in this study shows that it contains 22.43% Cr, 4.88% Ni, 3.13% Mo, 0.14% Mn, 0.67% Si, 0.18% N and 0.023% C by weight. This is the same material used during previous investigations that employed synchrotron radiation to observe phase transformations during welding [13,14]. The as-received material had been solution mill annealed at 1065 °C for 2.5 h followed by water quenching to produce a balanced ferrite/austenite microstructure. The sample was removed from a 10.8 cm diameter bar along the direction of extrusion, and had dimensions of 100 mm long by 4.75 mm wide and 2 mm thick. This is the same sample

* Corresponding author. Tel.: +1 925 422 6543; fax: +1 925 423 7040.
E-mail address: elmer1@llnl.gov (J.W. Elmer).

0921-5093/$ – see front matter © 2007 Elsevier B.V. All rights reserved.
doi:10.1016/j.msea.2007.01.071

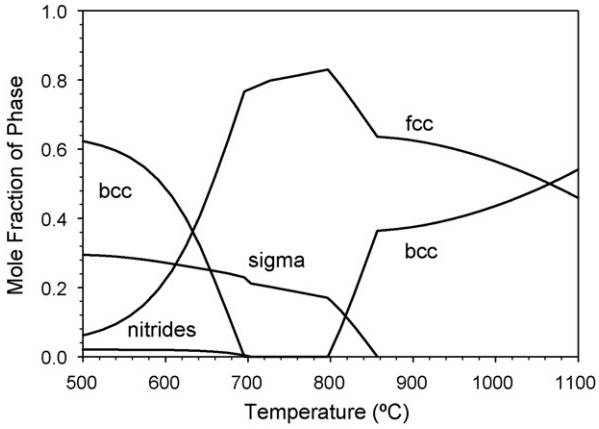

Fig. 1. Calculated phase fractions for the 2205 DSS alloy used in this study. The sigma phase is predicted to be present only at temperatures below 860 °C. The *y*-axis is plotted in mole fraction, where 1 mol is an Avogadro's number of total atoms.

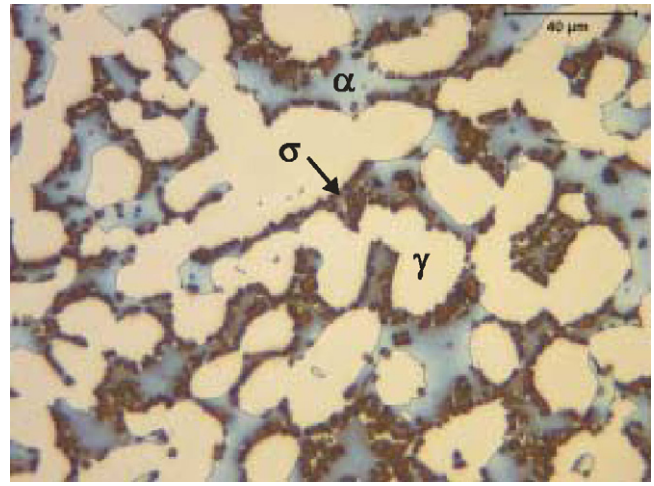

Fig. 2. Optical micrograph showing the microstructure of the sample after the heat treating cycle. Ferrite (α), austenite (γ), and sigma (σ) phase are indicated.

geometry and surface finish used in similar previous experiments [15,16]. The temperature was measured and controlled using 0.005 in. diameter Type S thermocouple wires that were spot welded to the back of the sample directly below the beam impingement point [15,16].

2.2. Thermodynamics

ThermoCalc® version q and the TC Fe2 database was used to calculate the phase equilibria in the 2205 DSS alloy. The model considered the effects of Fe, Cr, Ni, Mo, Mn, Si, C, and N, on the presence of ferrite, austenite, sigma, nitrides/carbides, and the liquid phases. Fig. 1 shows the calculated phase fraction plotted versus temperature, indicating that ferrite transforms to a combination of austenite and sigma during heating up to 700 °C. Between 700 and 800 °C the ferrite has completely transformed and is no longer present. At 800 °C ferrite begins to re-form, and sigma continues to decrease until it completely disappears at a temperature of approximately 860 °C. At higher temperatures, ferrite increases and austenite decreases until they have equal amounts at 1065 °C. Since the microstructure of the initial 2205 DSS is metastable due to its quenching from elevated temperatures, the real microstructure starts off with a significantly different ferrite/austenite ratio than that predicted from the thermodynamic calculations.

2.3. In situ X-ray diffraction experiments and data

The *in situ* X-ray diffraction was performed while heating test coupons in vacuum (10^{-4} Torr) using a direct resistance method [15–17]. The heating cycle consisted of a 20 °C/s ramp to the initial temperature of 850 °C where it was held for 30 min to form a measurable amount of sigma. The sample was then ramped to 1000 °C and back to 850 °C at a slow rate of 0.25 °C/s to determine the temperature where sigma dissolved. After ramping to and from 1000 °C, the sample was held at 850 °C for an additional 30 min to observe the re-formation of sigma before the sample was cooled back to room temperature at a rate of approximately 20 °C/s.

The microstructure of the DSS alloy is shown in Fig. 2 after the experiment. This sample was prepared by conventional metallographic polishing and etching in a KOH electrolyte (50 g KOH, 100 mL water) with a voltage of 3 V for approximately 10 s. In this micrograph, the austenite etches tan/white in color and the ferrite etches blue/purple in color. The sigma phase is the most darkly etched phase (brown/orange/black) in the microstructure.

In situ X-ray diffraction was performed at the Advanced Photon Source (APS) at the Argonne National Laboratory on the UNICAT beam line BM-33-C. This beam line produced a 30 keV X-ray beam that was adjusted to a size of 1.0 mm wide by 0.25 mm high using vertical and horizontal slits. A schematic diagram of the experimental setup is shown in Fig. 3,

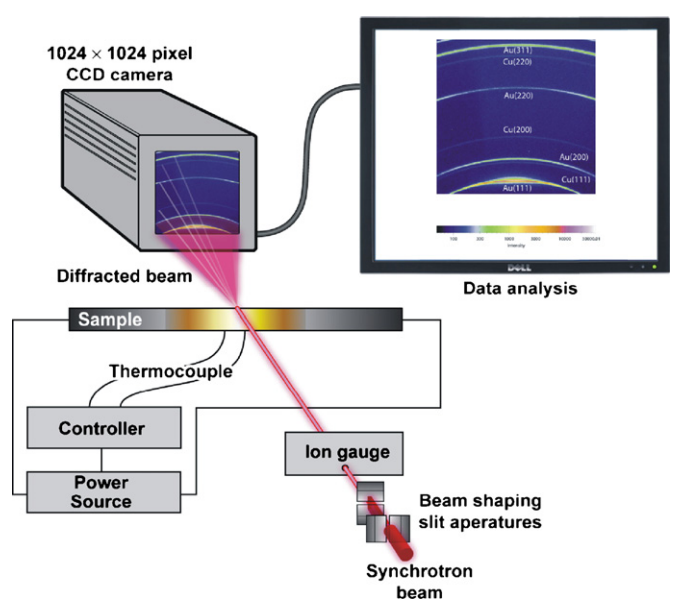

Fig. 3. Schematic diagram of the X-ray setup used for *in situ* observations of phase transformations under controlled heating and cooling conditions.

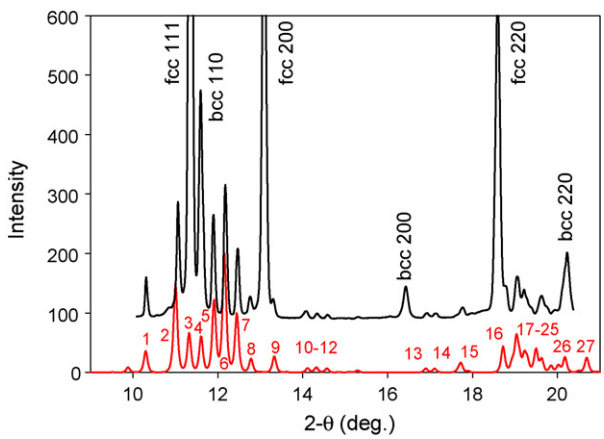

Fig. 4. Comparison of the measured room temperature diffraction pattern after heat treating showing bcc, fcc and sigma (upper line) with the calculated diffraction pattern of sigma (lower line).

where the X-ray beam impinges on the top surface of the sample at a 5° angle of incidence. Diffraction takes place on the surface of the sample and the diffracted beams are collected using a CCD detector manufactured by Roper Scientific (A99k401, RS/Photometrics) placed 330 mm behind the sample. This detector employs a 6.1 cm × 6.1 cm array of 1024 × 1024 pixels spaced 60 μm apart, and was programmed to integrate the diffraction patterns over a 1 s exposure time. The detector requires an additional 2 s to clear the data from the CCD array and transfer it to the computer. After the data was recorded, the Debye arcs were converted into a conventional diffraction plot to show the diffracted beam intensity versus *d*-spacing using Fit-2D software. Additional details about the data acquisition technique on this beam line are presented elsewhere [15–17].

Fig. 4 shows a room temperature diffraction pattern (upper line) taken after an 850 °C heat treatment where a significant amount of sigma phase had formed [7]. Superimposed on this figure is a calculated diffraction pattern of the sigma phase (lower line) [17]. The results show that three austenite peaks, three ferrite peaks, and a multitude of sigma phase peaks should appear in the diffraction window. All of the non-fcc or non-bcc peaks can be attributed to the sigma phase, and it can be seen that the sigma (3 3 0), peak 3, overlaps with the fcc (1 1 1), and that the sigma (2 0 2), peak 4, overlaps with the bcc (1 1 0) peaks. A complete indexing of all of the diffraction peaks for this DSS alloy is presented elsewhere [17].

Once all the X-ray diffraction data was acquired, the peak areas were measured for each phase and used as a means to determine their relative amounts. The peaks used in this measurement were the three major bcc peaks, (1 1 0), (2 0 0), (2 2 0), and the three major fcc peaks, (1 1 1), (2 0 0), (2 2 0). In addition, six of the highest *d*-spacing sigma peaks were analyzed corresponding to the (0 0 2), (4 1 0), (2 1 2), (4 1 1), (3 3 1), and (2 2 2) reflections. The diffraction peaks were then converted into phase fractions by taking into account the structure factors for ferrite, austenite, and sigma, the multiplicity for each peak, and the Lorentz polarization factors as described elsewhere [17]. These calculations were performed on every diffraction pattern throughout the isothermal hold, allowing the volume fraction of each phase to be determined during the heating cycle.

3. Results

Fig. 5 shows the data plotted for the initial 3700 s of the run, which includes the ramp to 1000 °C and back down to 850 °C. This figure shows the *d*-spacing range where the most important sigma peaks appear. The diffraction patterns are plotted with time along the *y*-axis, *d*-spacing along the *x*-axis, and the intensities of the diffraction peaks represented by different colors. The heating initiates at $t = 0$ s, and immediately all of the fcc and bcc diffraction peaks shift to higher *d*-spacings due to the thermal expansion effect while the sample is being heated to 850 °C. During holding at 850 °C, the intensity of the bcc peaks immediately begin to decrease while the intensity of the fcc peaks increase. At $t = 81$ s, the first sigma peak (4 1 1) appears, 40 s into the isothermal hold. With increased holding time this peak intensifies and additional sigma peaks develop. The ramp to 1000 °C begins at $t = 1850$ s, reaching 1000 °C at $t = 2450$ s. As the temperature ramps up to 1000 °C the amount of sigma decreases, eventually reaching 0% at a temperature of 985 °C. Sigma does not reappear again until the sample has been cooled back down to 850 °C.

Fig. 6 plots the remainder of the experiment, which shows the re-formation of sigma before the sample is cooled to room temperature. During this second hold at 850 °C, all of the sigma diffraction peaks gradually build in intensity, but never reach the high levels of intensity observed during the 850 °C hold before the temperature was ramped to 1000 °C. Upon cooling, which initiates at $t = 4850$ s, all of the diffraction peaks shift to lower *d*-spacing due to the thermal contraction effect and it is clear that some sigma is retained at room temperature.

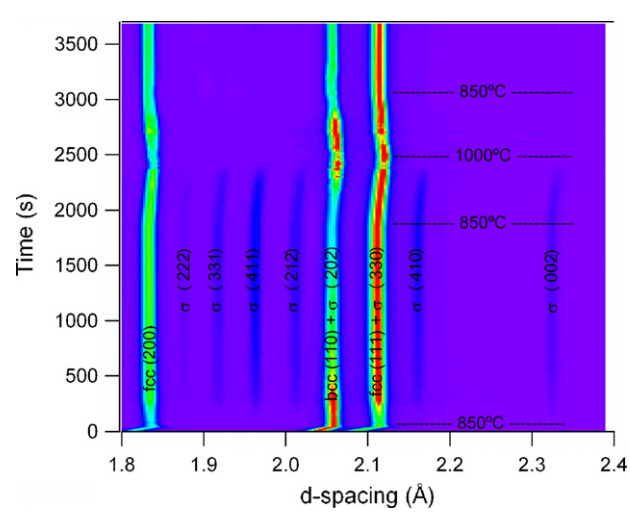

Fig. 5. X-ray diffraction sequence for the first 3700 s of the heat treatment. The red corresponds to the peak highest intensities and blue the lowest.

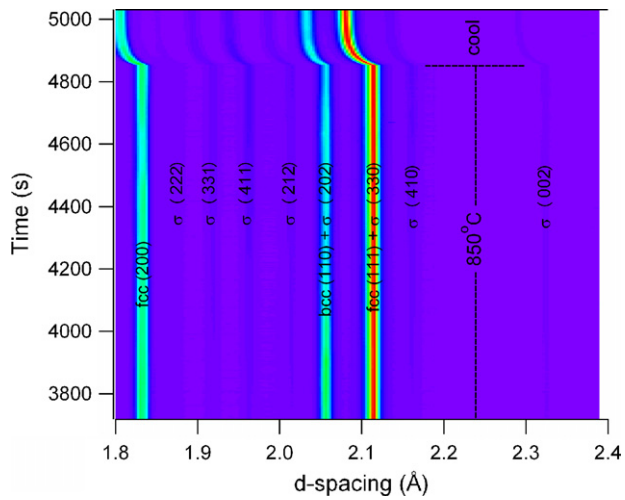

Fig. 6. X-ray diffraction sequence for the last 2200 s of the heat treatment, including the final cooling to room temperature.

4. Discussion

4.1. Sigma phase formation at 850 °C

Fig. 7 plots the measured volume fractions of the three phases as a function of time from the start to the end of the experiment. The alloy begins with a ferrite and austenite in nearly equal amounts, but this balance changes considerably as ferrite partially transforms to austenite and sigma phases during the isothermal hold at 850 °C. The sigma phase, which first appears at $t = 81$ s, increases to its highest value of 13.4% at $t = 1850$ s, just before the temperature begins to ramp up to 1000 °C. The highest amount of sigma observed here is consistent with the nose of the C-curve being at, or slightly below, 850 °C [17], and the rate of sigma formation is similar to the rate measured in a previous experiment on this alloy at 850 °C [17].

While the amount of sigma is increasing during the isothermal hold, the amount of ferrite decreases considerably from its initial value of 53.8% to its lowest value of 13.5% just before the temperature is increased. In addition, the amount of austenite increases from its initial value of 46.2–73.3% just before the temperature is increased.

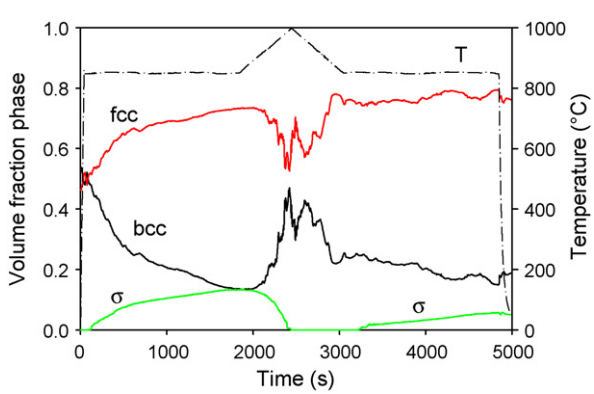

Fig. 7. Summary of the measured fractions of the ferrite (bcc), austenite (fcc) and sigma phases as a function of time from the start of the experiment. The temperature profile is indicated by the dashed line. Noise in the ferrite and austenite fractions appear at high temperatures when grain growth occurs and only a few grains satisfy the Bragg condition for diffraction.

4.2. Sigma phase dissolution

With 13.4% sigma created during the isothermal hold at 850 °C, the temperature was ramped to 1000 °C at 0.25 °C/s to observe the dissolution of sigma at higher temperatures. The thermodynamic calculations shown in Fig. 2 indicate that sigma should not be stable above 860 °C, and at this temperature sigma would be expected to dissolve fairly quickly. Although sigma immediately begins to decrease from its highest value as the temperature was increased above 850 °C (see Fig. 7), it does not disappear completely until 985 °C. This observed dissolution temperature for sigma is more than 100 °C higher that predicted by thermodynamics, and this difference can be explained by a combination of kinetic effects due to the heating rate, and possible inaccuracies in the thermodynamic calculations. In addition, errors in the temperature measurement will produce some errors that need to be taken into account.

The temperature measurement is accurate to a few degrees centigrade, and is made up of two factors. The first is the accuracy of the thermocouple, which is stated to be the larger of 0.25% of the measured value or 1.5 °C. This error becomes 2.5 °C at 1000 °C. The second factor is the uncertainty caused by the integration time of the X-ray detector while the sample is heating. This factor is estimated by the heating rate (0.25 °C/s) multiplied by the X-ray integration time (1 s), which is 0.25 °C. Adding the two errors together gives a total measurement uncertainty of the dissolution temperature of 2.75 °C, which is not believed to be a major contribution to the difference between the measured and calculated dissolution temperature difference.

The second contribution to the difference in the measured and calculated dissolution temperature is the accuracy of the thermodynamic calculations. Although this is not a known factor, there is evidence in the X-ray diffraction data that the thermodynamic calculations are underpredicting the dissolution temperature. Although the thermodynamics predicts the equilibrium fraction of sigma to be only 3.4% at 850 °C, 13.4% sigma is measured after 30 min of holding at this temperature, and even more is expected to form at longer holding times [17]. This difference between the measured and calculated amounts of sigma can be explained if the thermodynamics are underpredicting the sigma dissolution temperature. Another indication that the thermodynamics may not be completely accurate is that the measured ferrite and austenite values do not match up well with the calculations. For example, the thermodynamic calculations predict ferrite contents in excess of 20% at 850 °C, but the measured value was only 13% and was observed to be decreasing with additional holding time.

The third contribution to the difference between the measured and calculated amounts of sigma is the heating rate and other kinetic considerations such as surface versus bulk behaviors and inhomogeneous microstructural features. Although the heating rate of this sample is fairly slow at 0.25 °C/s, there will be some overshoot of the temperature above its equilibrium value due to

kinetics before sigma dissolves completely. Formation and dissolution of sigma requires diffusion of Cr and Mo, and may be seen from kinetics of sigma formation during isothermal holds, which is a slow process even at elevated temperatures [17]. With only one heating rate examined here, it is not possible to determine how much superheat can be attributed to the heating rate, and additional experiments are planned at different heating rates to study this effect.

4.3. Sigma phase re-formation after dissolution

As sigma dissolved at temperatures near 1000 °C, the amounts of ferrite and austenite fractions approached each other as expected. However, before this happened the volume fraction of ferrite and austenite trends became noisy, as seen in Fig. 7. This effect is most likely related to grain growth that is occurring at the high temperatures, which results in fewer grains satisfying the Bragg condition for diffraction and produces less perfect diffraction. As the temperature continued to decrease the noise reduced a bit as ferrite partially transformed to austenite. The final measurement shows a ferrite to austenite ratio of approximately 0.3, which is significantly lower that that of 0.54 at the beginning of the experiment.

The sigma phase was not observed to form during cooling from the peak temperature until 186 s after the 850 °C hold was reached. This time is more than four times longer than that required during the initial heating stage (40 s). In addition to the longer time required for sigma to appear, the rate of sigma formation was significantly reduced after cooling down from 1000 °C. As indicated in Fig. 7, 13.4% sigma was formed during the first 1800 s hold, whereas only 5.4% sigma formed during the same amount of time after cooling down from 1000 °C. The slower kinetics are most likely related to homogenization that takes place at the higher temperature which reduces the concentration gradients of Cr and Mo in the ferrite. In addition there is a probable decrease in the number of preferred nucleation sites for sigma since some grain growth would have taken place at 1000 °C to reduce the amount of grain and phase boundaries.

5. Conclusions

1. The formation and dissolution of sigma phase in 2205 duplex stainless steel was observed and measured in real time using synchrotron radiation to temperatures up to 1000 °C.
2. During the initial hold at 850 °C, 13.4% sigma formed in 30 min. This value is consistent with previous *in situ* observations of sigma formation at this temperature.
3. Dissolution of sigma at 850 °C was observed to occur at 985 ± 2.8 °C while heating at the rate of 0.25 °C/s. This temperature is more than 100 °C higher than the value predicted by thermodynamic calculations.
4. Differences between the calculated and measured sigma dissolution temperature were not fully resolved, however, it does appear that the thermodynamic calculations underpredict the actual dissolution temperature by a significant amount based on the amounts of sigma, ferrite, and austenite measured at 850 °C.
5. The kinetics of sigma formation at 850 °C were significantly slower after dissolution at 1000 °C than before. This change is most likely related to homogenization that took place at the peak temperature plus a reduction in the amount of preferred sigma nucleation sites.

Acknowledgements

The LLNL portion of this work was performed under the auspices of the U.S. Department of Energy, Lawrence Livermore National Laboratory, under contract no. W-7405-ENG-48. The ORNL portion of this work was sponsored by the U.S. Department of Energy Division of Materials Sciences and Engineering under contract no. DE-AC05-00OR22725 with UT-Battelle, LLC. The UNICAT facility at the Advanced Photon Source (APS) is supported by the U.S. DOE under award no. DEFG02-91ER45439, through the Frederick Seitz Materials Research Laboratory at the University of Illinois at Urbana-Champaign, the Oak Ridge National Laboratory (U.S. DOE contract DE-AC05-00OR22725 with UT-Battelle, LLC), the National Institute of Standards and Technology (U.S. Department of Commerce) and UOP LLC. The APS is supported by the U.S. DOE, Basic Energy Sciences, Office of Science under contract no. W-31-109-ENG-38. The authors would like to thank Mr. Jackson Go for performing the optical metallography.

References

[1] H.D. Solomon, T.M. Devine, in: R.D. Lula (Ed.), Duplex Stainless Steels, American Society for Metals, Metals Park, OH, 1983, pp. 693–756.
[2] L. Karlsson, WRC Bull. 438 (1999).
[3] J.-O. Nilsson, Mater. Sci. Technol. 8 (1992) 685–700.
[4] E.O. Hall, S.H. Algie, Metallurgical Reviews. Review No. 104, vol. 11, The Institute of Metals, 1966, pp. 61–88.
[5] J.-O. Nilsson, P. Kangas, T. Karlsson, A. Wilson, Metall. Mater. Trans. A 31A (2000) 35–45.
[6] J.-O. Nilsson, A. Wilson, Mater. Sci. Technol. 9 (1993) 545–554.
[7] Y.S. Ahn, M. Kim, B.H. Jeong, Mater. Sci. Technol. 18 (2002) 383–388.
[8] E. Johnson, Y.-J. Kim, L.S. Chumbley, B. Gleeson, Scripta Mater. 50 (2004) 1351–1354.
[9] Y.-J. Kim, L.S. Chumbley, B. Gleeson, Metall. Mater. Trans. A 35A (2004) 3377–3386.
[10] J.M. Vitek, S.A. David, Metall. Trans. A 18A (1987) 1195–1201.
[11] T.H. Chen, J.R. Yang, Mater. Sci. Eng. A 338 (2002) 166–181.
[12] T.H. Chen, J.R. Yang, Mater. Sci. Eng. A 311 (2001) 28–41.
[13] T.A. Palmer, J.W. Elmer, S.S. Babu, Mater. Sci. Eng. A 374 (2004) 307–321.
[14] T.A. Palmer, J.W. Elmer, J. Wong, Sci. Technol. Weld. Join. 7 (3) (2002) 159–171.
[15] J.W. Elmer, T.A. Palmer, S.S. Babu, E.D. Specht, Mater. Sci. Eng. A 391 (1/2) (2005) 104–113.
[16] J.W. Elmer, T.A. Palmer, S.S. Babu, E.D. Specht, Scripta Mater. 52 (10) (2005) 1051–1056.
[17] J.W. Elmer, T.A. Palmer, E.D. Specht, Metall. Mater. Trans. A, in press.